

# Multilevel Pulse-Position Modulation Based on Balanced Incomplete Block Designs

Mohammad Noshad and Maïté Brandt-Pearce

Charles L. Brown Department of Electrical and Computer Engineering

University of Virginia

Charlottesville, VA 22904

Email: mn2ne@virginia.edu, mb-p@virginia.edu

**Abstract**—In this paper, two new modulation schemes using multilevel pulse-position modulation (PPM) for application in unipolar optical wireless systems are presented. Balanced incomplete block designs (BIBD) are used for constructing the symbol alphabets. Each symbol is obtained by combining multiple codewords of a BIBD code. In one scheme the symbols have equal energies, and therefore, no threshold is needed to make a decision on the received signal. The other modulation has better performance yet higher complexity. Since cyclic BIBDs are used for constructing the symbols, the transmitters and receivers have simple structures, and can be implemented using shift registers. These schemes can achieve high spectral-efficiencies, and are therefore suitable for systems with bandlimited sources or highly dispersive channels, where intersymbol interference (ISI) has a significant impact on the performance. We also show that using the same receiver structure, the constellation size can be increased by including the complements of the codewords. The performance of the proposed schemes are compared to other modulation schemes for both LED-based non-dispersive and dispersive free-space optical (FSO) systems.

**Index Terms**—Multilevel modulation, pulse position modulation (PPM), balanced incomplete block design (BIBD), free space optical (FSO) systems, spectral-efficiency

## I. INTRODUCTION

Free space optical (FSO) communications has recently attracted significant interest because of its huge unlicensed bandwidth and potential in providing high data-rates [1], [2]. Emerging applications, such as indoor visible light optical communications and non-line-of-sight (NLOS) ultraviolet (UV) communications [3], have made FSO communications more important than ever. Pulse position modulation (PPM) is considered the primary  $M$ -ary transmission technique for FSO links, since it can be implemented incoherently and does not need a threshold to make decisions at the receiver side, which is important in fading channels. Because of the low spectral-efficiency of PPM, dispersive channels cause interference between the time-slots. Therefore, low spectral-efficiency is the main limiting factor for PPM, which makes it vulnerable to intersymbol interference (ISI), and prevents it from being used in dispersive channels, such as in the applications mentioned above. Multipulse PPM (MPPM) has been proposed [4] to improve the spectral-efficiency of PPM by increasing the constellation size. In this paper, we propose two new multilevel pulse-position based modulation schemes to achieve higher spectral-efficiencies while simultaneously

enforcing large minimum pairwise Hamming distances between symbols.

Various multilevel modulation schemes using a combination of PPM and pulse-amplitude modulation (PAM) have been proposed in the literature in order to improve the spectral-efficiency of pulse-position based modulations [5], [6], [7]. In these works, all combinations of PPM and PAM are considered as symbols, and therefore, the minimum distance between symbols is small. Moreover, the symbols in these schemes contain different energies, and hence the receiver requires a threshold value to make a decision, which is a disadvantage in fast-fading channels.

In [8], we propose a novel unipolar modulation scheme, called expurgated PPM (EPPM), as an alternative technique to PPM to improve the performance of peak-power limited  $M$ -ary communication systems. Balanced incomplete block designs (BIBD) are used as modulated symbols in order to increase the Hamming distance between symbols. Because of the cyclic structure of the BIBD codes, the transmitter and receiver have low complexity and can be implemented using shift registers. It is also shown that for the same receiver structure, by including the complements of the codewords a higher constellation size can be achieved.

In our proposed modulation schemes, the multilevel symbols are obtained as linear combinations of BIBD codewords, and therefore, all symbols have fixed weight. These techniques can be considered as multilevel forms of EPPM, and thus, we call them multilevel EPPM (MEPPM). We propose two constructions of MEPPM: one with a simpler decoder and no need for a threshold, and the other with better performance in exchange for a somewhat more complex detector. We also show that by including the complements of the BIBD codewords the constellation size can be increased significantly, without any change in the receiver structure. The proposed technique can achieve 75% higher spectral-efficiency compared to MPPM at a BER of  $10^{-5}$ .

The rest of the paper is organized as follows. Section II describes the principles of the MEPPM schemes and the transmitter and receiver structures. The analytical symbol error probability of MEPPM is approximated in Section III using the union bound, and the spectral-efficiency is calculated for each scheme. Numerical results are presented in Section IV, and the spectral-efficiencies of our proposed multilevel schemes are compared with other modulations. Finally, conclusions are

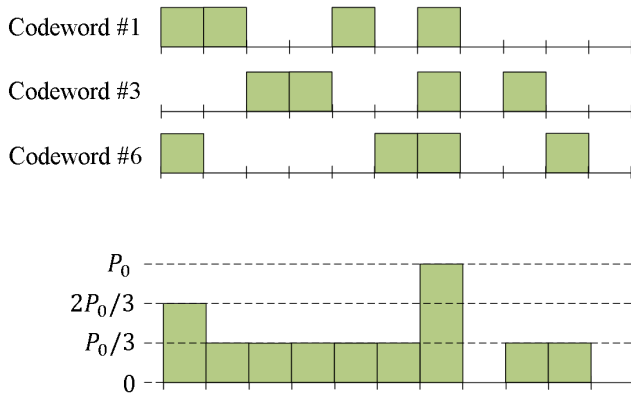


Fig. 1. A 4-level EPPM symbol constructed using codewords 1, 3 and 6 of a (11, 4, 1)-BIBD.

provided in Section V.

## II. PRINCIPLES OF MULTILEVEL EPPM

This section explains the principles of the multilevel EPPM (MEPPM) and its transmitter/receiver structures. In these schemes, similar to PPM, the symbol period is divided into  $Q$  equal time-slots. A unipolar  $L$ -level encoding is applied on the amplitude of the optical power in each time-slot. Hence, symbol  $k$  is denoted by  $S_k = (s_{k1}, s_{k2}, \dots, s_{kQ})$ , where  $0 \leq s_{ki} \leq L - 1$ .

We use the codewords of a BIBD code to construct the symbols of MEPPM. A BIBD code is composed of  $Q$  codewords,  $\{C_1, C_2, \dots, C_Q\}$ , and each codeword has a length of  $Q$ , i.e.,  $C_j = (c_{j1}, c_{j2}, \dots, c_{jQ})$  [9],  $c_{ji} \in \{0, 1\}$ , such that

$$\sum_{i=1}^Q c_{ji} c_{ki} = \begin{cases} K & ; j = k, \\ \lambda & ; j \neq k \end{cases}, \quad (1)$$

where  $K$  is the weight and  $\lambda$  is the cross-correlation of that code. We denote a BIBD code by  $(Q, K, \lambda)$ , and the following relation holds for its parameters [9]:

$$\lambda(Q - 1) = K(K - 1). \quad (2)$$

For our MEPPM, each symbol is obtained as the sum of  $N$  BIBD codewords from the same code, resulting in new length- $Q$  codewords. We focus on cyclic BIBDs, for which the codewords are cyclic shifts of each other. To build symbol  $k$ ,  $N$  codewords are chosen, denoted as  $C_{k_n}$ ,  $n = 1, 2, \dots, N$ ,  $k_n \in \{1, 2, \dots, Q\}$ , resulting in  $S_k = (s_{k1}, s_{k2}, \dots, s_{kQ})$ , where  $s_{ki}$  can be obtained as

$$s_{ki} = \sum_{n=1}^N c_{k_n i}. \quad (3)$$

According to this definition, the symbols of a MEPPM constellation have equal weight, where the weight of each symbol is  $NK$ . Fig. 1 shows the generation of a MEPPM symbol from 3 BIBD codewords ( $N = 3$ ). In this example, codewords  $C_1$ ,  $C_3$  and  $C_6$  of a (11, 4, 1)-BIBD code are added to create a symbol with length 11 and weight 12.

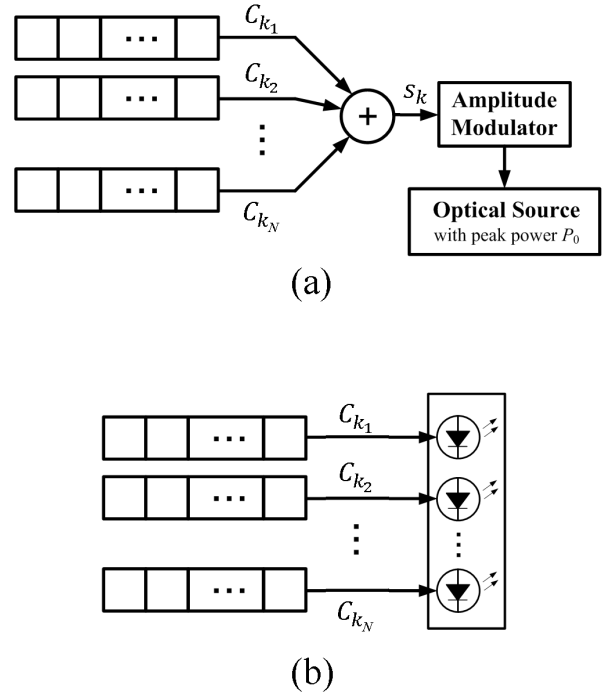


Fig. 2. Transmitter structure and symbol generation using  $N$  shift registers and using (a) a multilevel optical source such as laser, (b) an LED-array.

Since the BIBD code used to generate the multilevel symbols is assumed to be cyclic, the symbol generator circuit at the transmitter can be implemented using  $N$  shift registers in  $N$  branches, as depicted in Fig. 2. In the general case, the number of branches,  $N$ , can be different from the number of levels,  $L$ . The optical source in the transmitter can be either a laser or an LED-array. Therefore, there can be two structures for the transmitter. In the first structure, as shown in Fig. 2-(a), each shift register generates one BIBD codeword, and then the outputs of these  $N$  branches are added to generate the corresponding  $L$ -level symbol. The symbol generated is applied to an external amplitude modulator, which modulates the output power of the optical source. Lasers used as transmitters of FSO systems are peak power limited sources, and we assume the output optical power can be modulated between 0 and  $P_0$ . The number of power levels is flexible. For symbol  $S_k$ , the output power of the source in time-slot  $i$  is  $s_{ki}P_0/(L - 1)$ .

An LED-array is the other option for an optical source used in FSO links for which accurate pointing is less critical. Ultraviolet (UV) communications [10] and indoor FSO systems [11] are two emerging technologies that can use LED-arrays as optical sources at the transmitter. In an LED-array, each LED can be turned on and off independently, and hence, the whole array can be considered as a multilevel source. Thus, it can be used directly as the optical source in Fig. 2-(a). Alternatively, the transmitter using an LED-array can be implemented as in Fig. 2-(b), in which each codeword is directly sent to a subset LEDs in the array, and hence, it is simpler than the structure in Fig. 2-(a). The array size determines the maximum number of levels, and  $L - 1$  should be a divisor of the array size.

In MEPPM, each set of  $N$  BIBD codewords determines

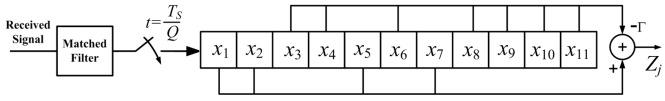


Fig. 3. Receiver for the MEPPM code shown in Fig. 1.  $T_s$  is the symbol period.

one symbol. Thus, as in EPPM, the front-end of the optimal receiver, assuming an additive Gaussian noise, can be implemented using a shift register with length  $Q$  [8], as shown in Fig. 3. In this figure,  $\Gamma$  is  $\frac{\lambda}{K-\lambda}$ . The receiver generates  $Q$  variables in each symbol period at the output of the differential circuit by circulating  $X = \{x_1, x_2, \dots, x_Q\}$ , the received data stored in the shift register. The combination of the shift register and the differential circuit generates the decision statistic  $z_j = \langle X, C_j \rangle - \Gamma \langle X, \bar{C}_j \rangle$ , for  $j = 1, 2, \dots, Q$ , where  $\langle X, Y \rangle$  denotes the dot product of the vectors  $X$  and  $Y$ . Hence, the  $z_j$ 's form a sufficient statistic for detection.

Due to the fixed cross-correlation property of the BIBD codewords, assuming that  $C_\ell$  is transmitted, its contribution in the expected value of  $z_\ell$  is  $E\{z_\ell\} = \frac{\mathcal{E}}{L-1}K$ , and in  $z_j$ ,  $j \neq \ell$ , is  $E\{z_j\} = 0$  [12], where  $\mathcal{E}$  is the received energy in one time-slot for an unmodulated transmitted signal with peak power  $P_0$ .

Depending on whether the codewords used in the generation of the symbols must be distinct or not, MEPPM can be categorized into two types, discussed below.

#### A. Type I Multilevel EPPM

For this scenario, the  $N$  branches generate distinct codewords, and each codeword is used at most once in the generation of each symbol, i.e.,  $k_n \neq k_m$  for  $\forall n \neq m$ . Hence, the total number of symbols for type I MEPPM with  $N$  branches is  $\binom{Q}{N}$ . This constellation size is maximized for  $N = Q/2$ .

For this case, the energy of the symbol  $S_k$  is

$$|S_k|^2 = \left| \sum_{n=1}^N C_{k_n} \right|^2 = \sum_{n=1}^N |C_{k_n}|^2 + \sum_{n=1}^N \sum_{\substack{m=1 \\ m \neq n}}^N \langle C_{k_n}, C_{k_m} \rangle, \quad (4)$$

which, using (1), becomes  $|S_k|^2 = NK + N(N-1)\lambda$ , for  $\forall k$ . Hence, all symbols have equal energy in type I MEPPM. For the receiver in Fig. 3, when symbol  $k$  is transmitted, we get  $E\{z_j\} = \frac{\mathcal{E}}{L-1}K$  for  $j \in \{k_1, k_2, \dots, k_N\}$ , and  $E\{z_j\} = 0$  for  $j \notin \{k_1, k_2, \dots, k_N\}$ . Thus, by finding the  $N$  largest  $z_j$ 's we make an optimal decision on the received symbol. This detector does not require any threshold or energy compensation to make a decision.

In a  $(Q, K, \lambda)$ -BIBD code, the number of codewords that have "1" in a specific position is  $K$ . Therefore, for symbols composed of  $N$  different codewords, each element is less than or equal to  $K$ , i.e.  $s_{ki} \leq K$  for  $\forall k, i$ . Hence, for type I, we have

$$L-1 \leq \min\{N, K\}. \quad (5)$$

For  $N \geq K$ , which is typical, we have  $L = K + 1$ .

For a Gaussian additive noise channel, the symbol error probability is a function of the Euclidean distance between the symbols. Since the Hamming distance between the codewords of a  $(Q, K, \lambda)$ -BIBD code is  $2(K-\lambda)$ , the minimum Euclidean distance between the symbols of type I MEPPM is

$$d_{\min}^E = \frac{\mathcal{E}}{K} 2(K-\lambda), \quad (6)$$

which, using (2), becomes

$$d_{\min}^E = 2\mathcal{E}\left(1 - \frac{K-1}{Q-1}\right). \quad (7)$$

This distance takes its maximum value for  $K = 1$ , which corresponds to using PPM constituent codewords. This means that the minimum error probability is achieved when the generating codewords are the symbols of the PPM scheme. For this case, type I MEPPM reduces to multipulse PPM (MPPM). When spectral-efficiency is important, the  $Q = 2K + 1$  case is used since the complements of the codewords can also be included as codewords, but when power-efficiency is important, MPPM is preferred over type I MEPPM.

#### B. Type II Multilevel EPPM

In this case, different branches are allowed to have the same codewords, i.e., one codeword can be used more than once in the generation of each symbol. To calculate the constellation size, let  $n_k$  be the number of branches that have codeword  $C_k$ , where  $0 \leq n_k \leq N$ , then we have

$$\sum_{k=1}^Q n_k = N. \quad (8)$$

The energy of the symbol  $S_k$  for this type is

$$|S_k|^2 = \left| \sum_{k=1}^Q n_k C_k \right|^2 = \sum_{k=1}^Q n_k^2 |C_k|^2 + \sum_{k=1}^Q \sum_{\substack{\ell=1 \\ \ell \neq k}}^Q n_k n_\ell \langle C_k, C_\ell \rangle. \quad (9)$$

Using (1) and (8), we get

$$|S_k|^2 = (K-\lambda) \sum_{k=1}^Q n_k^2 + \lambda N^2. \quad (10)$$

As one can see, for type II MEPPM, the symbols do not have equal energies, and therefore, we need an energy compensator to make an optimal decision. For this type, the outputs of the receiver in Fig. 3 are  $E\{z_j\} = \frac{\mathcal{E}}{L-1}n_j K$ . The optimal detector can be implemented as

$$\max_{n_1, n_2, \dots, n_Q} \sum_{k=1}^Q n_k \langle X, C_k \rangle - (K-\lambda) \left( \frac{\mathcal{E}}{L-1} \right)^2 \sum_{k=1}^Q n_k^2. \quad (11)$$

Using the definition of  $z_k$ , the detector becomes

$$\max_{n_1, n_2, \dots, n_Q} \sum_{k=1}^Q \left( z_k - \mathcal{E} \frac{K}{L-1} n_k \right)^2 \quad (12)$$

We can use an iterative decoder to find the optimal  $n_j$ 's. In order to make an optimal decision, we define  $w_j^{[m]}$  as the hypothesized  $n_j$  at iteration  $m$ , with initial value of  $w_j^{[0]} = 0$ . In each iteration, we update the weights as follows

$$w_j^{[m+1]} = \begin{cases} w_j^{[m]} + 1 & j = \arg \max_{1 \leq k \leq Q} \left\{ z_k - w_k^{[m]} \mathcal{E} \frac{K}{L-1} \right\}, \\ w_j^{[m]} & \text{otherwise.} \end{cases} \quad (13)$$

At step  $m = N$ , we set  $n_j = w_j^{[m]}$ . The most likely symbol sent uses  $n_k$  copies of  $C_k$ ,  $k = 1, 2, \dots, Q$ , assuming an additive white Gaussian noise (AWGN) channel.

The constellation size is equal to the number of solutions of (8), which is equal to  $\binom{Q+N}{N}$ . As can be seen, the constellation size for type II is larger than that of the type I, leading to a more spectrally efficient design. In contrast, it requires a more complicated receiver compared to type I.

We define  $M_\ell$  as the number of symbols generated from exactly  $\ell$  distinct codewords, which is equal to the number of integer solutions of

$$n_{k_1} + n_{k_2} + \dots + n_{k_\ell} = N, \quad (14)$$

where  $k_j \in \{1, 2, \dots, Q\}$  for  $j = 1, 2, \dots, \ell$ . The number of solutions to (14) is

$$M_\ell = \binom{Q}{\ell} \binom{N-1}{\ell-1}. \quad (15)$$

For type II MEPPM, the number of levels,  $L$ , is  $N + 1$ , independent from  $K$ . The minimum Euclidean distance for this case is

$$d_{\min}^E = 2 \frac{\mathcal{E}}{N} K \left( \frac{Q-K}{Q-1} \right). \quad (16)$$

As this discussed in [8], the optimum parameters to maximize  $d_{\min}^E$  in (16) are  $Q = 2K + 1$  and  $K = 2\lambda + 1$ .

### C. Multilevel Augmented EPPM

For a BIBD code with  $Q = 2K + 1$  and  $K = 2\lambda + 1$ , the Hamming distance between  $\overline{C}_j$ , the complement of  $C_j$ , and  $C_i$  is [8]

$$d(\overline{C}_j, C_i) = \begin{cases} Q & ; i = j, \\ 2\lambda + 1 & ; i \neq j. \end{cases}$$

Thus, the complements of codewords can also be included as symbols in EPPM with only a minor penalty on the minimum distance. The new scheme that is obtained by including the complements of codewords is called augmented EPPM (AEPPM) in [8]. Similarly, we can increase the constellation size using these complements in MEPPM. To do this, in Fig. 2, we first choose  $N$  codewords out of  $Q$ , and then in each branch we choose between the codeword and its complement. We call this scheme multilevel AEPPM (MAEPPM). In this way the constellation size for type I can be increased to  $2^N \binom{Q}{N}$ . For type II MAEPPM, using this approach the number of symbol generated from  $\ell$  distinct codewords can be increased from  $M_\ell$  to  $2^\ell M_\ell$ . So, the total number of symbols for type II MAEPPM

is equal to

$$M = \sum_{\ell=1}^N 2^\ell \binom{Q}{\ell} \binom{N-1}{\ell-1} = P_N^{(Q-N, -1)}(3), \quad (17)$$

where  $P_n^{(\alpha, \beta)}(x)$  is the Jacobi polynomial [13].

For MAEPPM the same receiver as Fig. 3 is used, and a similar decoding is applied to detect the symbol sent, except that, instead of the set  $\{z_1, z_2, \dots, z_Q\}$ , we form the set  $\{z_1, z_2, \dots, z_Q, -z_1, -z_2, \dots, -z_Q\}$  [8], and make a decision using this set.

### III. ERROR PERFORMANCE AND SPECTRAL-EFFICIENCY

In this section we obtain expressions for the symbol error probability for the modulation schemes described in Section II. We use the resulting expressions to derive the spectral-efficiency of the various schemes. We assume an additive white Gaussian noise channel with power spectral density  $N_0/2$ , as appropriate for thermal or background noise limited FSO systems. We model the effect of this noise by adding a Gaussian random variable with variance  $\Delta f N_0$  to the decision statistic  $z_j$ ,  $j = 1, 2, \dots, Q$ , where  $\Delta f$  is the receiver bandwidth. Therefore, the optimum maximum likelihood (ML) decision rule reduces to the minimum distance criterion. For type I, since the energies of the symbols are the same, the performance of the correlation receiver in Fig. 3 is optimal. The union bound on the symbol error probability for an  $M$ -ary modulation can be expressed as [14, p. 334]

$$P_s^{(U)} = \frac{1}{2M} \sum_{i=1}^M \sum_{\substack{j=1 \\ i \neq j}}^M \text{erfc} \left( \sqrt{\frac{d_{ij}^H \gamma}{2(L-1)} \frac{\log_2 M}{Q}} \right). \quad (18)$$

where  $d_{ij}^H$  is the Hamming distance between symbols  $i$  and  $j$ . For an FSO system with bit-rate  $R_b$ , received peak optical power  $P_r$  (unmodulated) and photodetector responsivity  $\rho$ , we define the peak SNR as  $\gamma = \frac{\rho^2 P_r^2}{N_0 R_b}$ . For high SNRs, the smallest Hamming distance between symbols,  $d_{\min}^H$ , limits  $P_s$ , so (18) is approximated by

$$P_s^{(U)} \approx \frac{M'}{2M} \text{erfc} \left( \sqrt{\frac{d_{\min}^H \gamma}{2(L-1)} \frac{\log_2 M}{Q}} \right), \quad (19)$$

where  $M'$  is the number of symbol pairs with Hamming distance  $d_{\min}^H$ .

For type I MEPPM, we have  $M = \binom{Q}{N}$  and, therefore, its spectral-efficiency is

$$\eta_{1, \text{MEPPM}} = \frac{\log_2 \binom{Q}{N}}{Q}. \quad (20)$$

The smallest Hamming distance between symbols is  $d_{\min}^H = 2(K - \lambda)$  and  $M' = \frac{N(Q-N)}{2} \binom{Q}{N}$ . MPPM is a special case with  $K = 1$  and  $\lambda = 0$ .

For type II MEPPM, the constellation size is  $M = \binom{Q+N}{N}$ , and hence, we have

$$\eta_{2, \text{MEPPM}} = \frac{\log_2 \binom{Q+N}{N}}{Q}. \quad (21)$$

For this type,  $d_{\min}^H = 2(K - \lambda)$  and, for a symbol composed of  $\ell$  distinct codewords, the number of pairs of symbols with Hamming distance  $2(K - \lambda)$  is  $\ell(Q - \ell)$ . Hence, the total number of symbol pairs with distance  $2(K - \lambda)$  is

$$M' = \frac{1}{2} \sum_{\ell=1}^N \ell(Q - \ell)M_\ell = \frac{Q(Q - 1)}{2} \binom{Q + N - 3}{N - 1}. \quad (22)$$

For type I and type II MAEPPM, the minimum Hamming distance decreases to  $d_{\min}^H = 2\lambda + 1$ , and the spectral-efficiencies are

$$\eta_{1, \text{MAEPPM}} = \frac{N + \log_2 \left( \frac{Q}{N} \right)}{Q}, \quad (23)$$

and

$$\eta_{2, \text{MAEPPM}} = \frac{\log_2 P_N^{(Q-N, -1)}(3)}{Q}, \quad (24)$$

respectively.

To calculate the BER, we denote the assigned  $(\log_2 M)$ -bit binary sequence to symbol  $k$  by  $\mathbf{b}_k$ . When the transmitted symbol  $k$  is estimated incorrectly as symbol  $k'$ ,  $d(\mathbf{b}_k, \mathbf{b}_{k'})$  bits are decoded incorrectly. Hence, for an  $M$ -ary modulation scheme, an upper bound on the BER is given by [14]

$$P_b^{(U)} = \frac{1}{2M} \sum_{k=1}^M \sum_{\substack{k'=1 \\ k' \neq k}}^M \text{erfc} \left( \sqrt{\frac{d_{kk'}^H \gamma}{2(L-1)} \frac{\log_2 M}{Q}} \right) \frac{d(\mathbf{b}_k, \mathbf{b}_{k'})}{\log_2 M}. \quad (25)$$

For all proposed multilevel schemes, the optimum bit-symbol mapping is similar to MPPM, and is a difficult problem. Hence, in our work, we use a random bit-symbol mapping, for which the BER is  $P_s^{(U)}/2$ .

#### IV. NUMERICAL RESULTS

In this section, numerical results are presented to compare the performance of MEPPM and MAEPPM with other schemes. We use Paley, projective geometry (PG) and twin prime power (TPP) difference sets [9] as BIBD code families in these results, as for these code families  $Q = 2K + 1$  and  $K = 2\lambda + 1$ .

Fig. 4 shows the spectral-efficiency from (20)-(24) versus the required peak SNR,  $\gamma$ , for a BER of  $10^{-5}$ , for OOK, PAM, MPPM, type I and II MEPPM, and type I and type II MAEPPM from (19) and (25). Each point represents a scheme with different parameters. For all multilevel modulation schemes,  $N = (Q - 1)/2$  and  $Q$  is 7, 11, 19, 35, 67, 131 and 263. MPPM, MEPPM and MAEPPM are able to achieve high spectral-efficiencies since their constellation sizes are large. From these plots, the spectral-efficiency is the same for MPPM and type I MEPPM, but MPPM requires a lower  $\gamma$ . Among all pulse-position based schemes type II MAEPPM is the most efficient modulation for spectrum usage. Type II MAEPPM is able to achieve 75% higher spectral-efficiency compared to MPPM with only a small SNR penalty.

The symbol error probability of PPM, EPPM, MPPM, MEPPM and MAEPPM are compared for a fixed bit-rate in Fig. 5 for an FSO link. For all these schemes  $Q = 19$  and

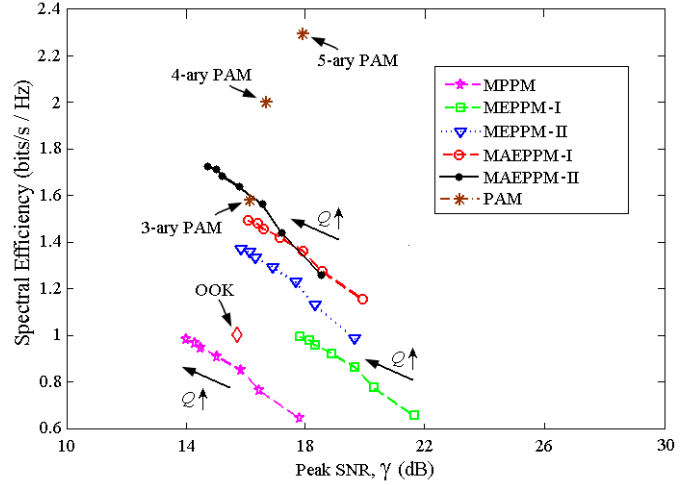


Fig. 4. Analytical spectral-efficiency and required  $\gamma$  for BER of  $10^{-5}$ , for OOK, PAM, MPPM, type I and type II MEPPM, and type I and type II MAEPPM.

$N = 9$ , and for MEPPM and MAEPPM a (19,9,4)-BIBD code is used. According to these results, EPPM has the best performance among all techniques.

To test the performance of our modulation scheme in a dispersive environment in the absence of an equalizer, the BER of on-off keying (OOK), PAM, EPPM and type II MAEPPM schemes are compared in Fig. 6 for a dispersive FSO link. A practical example of a dispersive FSO link is non-line of sight ultraviolet (NLOS-UV) communications [15]. For this FSO link, the channel impulse response is assumed to be Gaussian with broadening factor  $\sigma$ , i.e.  $h(t) = \frac{1}{\sqrt{2\pi}\sigma} \exp(-t^2/2\sigma^2)$ . Here we assume  $\gamma$  is 16 dB. For EPPM and type II MAEPPM, a BIBD code with  $Q = 19$ ,  $K = 9$  and  $\lambda = 4$  is used. The BERs are plotted versus the normalized broadening factor,  $\sigma R_b$ , where  $R_b$  is the bit-rate. The transmitted signal is assumed to have a non-return-to-zero rectangular pulse

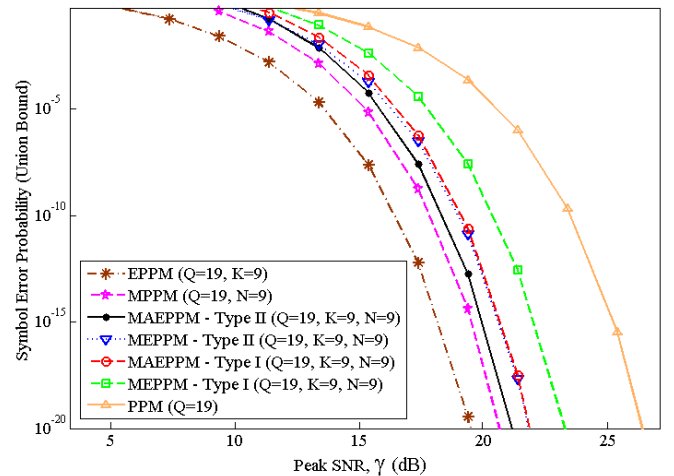


Fig. 5. Union bound on symbol error probability of an FSO link versus  $\gamma$  for PPM, EPPM, MPPM ( $N = 9$ ), type I and type II MEPPM ( $N = 9$ ), and type I and type II MAEPPM ( $N = 9$ ). For all these schemes  $Q = 19$ .

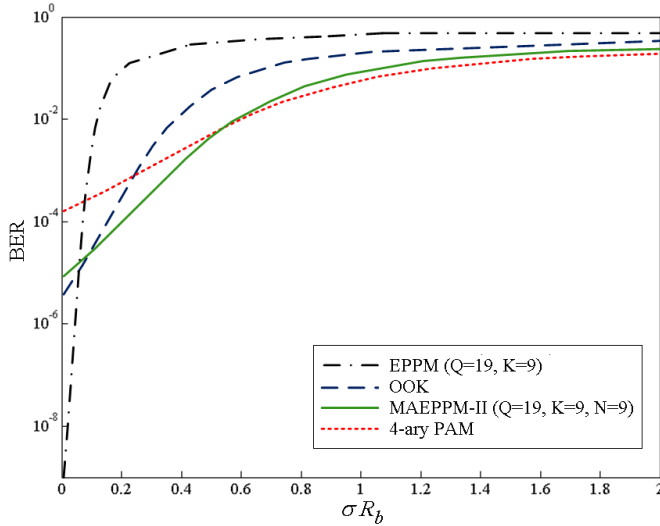


Fig. 6. Simulated BER vs. normalized broadening factor for a FSO link for OOK, EPPM, type I MAEPPM and 4-ary PAM.

shape, and the received pulse is obtained by convolving the transmitted signal with the channel impulse response. By increasing  $\sigma R_b$ , the ISI effect becomes the dominant limit, and, therefore, schemes with higher spectral-efficiencies perform better. Although EPPM has the lowest BER for non-dispersive channels, it is the most vulnerable scheme to ISI since it has the lowest spectral-efficiency. On the other hand, while 4-ary PAM has the best performance in high dispersive channels, because of its low BER at  $\sigma = 0$ , it is not the best technique for low dispersive channels. Type II MAEPPM has the best performance for medium dispersion cases, and suffers only a small performance penalty compared to 4-PAM in high dispersion cases.

## V. CONCLUSION

In this paper, novel modulation schemes called multilevel expurgated PPM are proposed. The symbols are constructed by combining several BIBD codewords. Indeed, the symbols of these schemes can be considered as a subset of combined PPM-PAM symbols. Because of the large constellation sizes that can be achieved, the proposed schemes are more spectrally efficient than MPPM, PPM and EPPM. Simple transmitter and receiver structures using shift registers are presented. MEPPM is divided into two types, based on the variety of the codewords that can be considered in the generation of the symbols. It is shown that by adding the complements of the BIBD codewords, a larger constellation size can be attained

for the same transmitter/receiver structures. Analytical symbol error probabilities and spectral-efficiencies are calculated, and numerical results are presented to compare the performance of the proposed schemes with other modulation techniques. The application of MEPPM and MAEPPM in dispersive FSO channels is also discussed, and their performances are compared with OOK and PAM. The proposed schemes are shown to outperform existing techniques over dispersive channels.

## VI. ACKNOWLEDGMENT

This research was funded by the National Science Foundation (NSF) under grant number ECCS-0901682.

## REFERENCES

- [1] K. Kiasaleh, "Performance of APD-based, PPM free-space optical communication systems in atmospheric turbulence," *IEEE Trans. Commun.*, vol. 53, no. 9, pp. 1455–1461, 2005.
- [2] S. G. Wilson, M. Brandt-Pearce, Q. Cao, and J. H. Leveque, "Free-space optical MIMO transmission with  $Q$ -ary PPM," *IEEE Trans. Commun.*, vol. 53, no. 8, pp. 1402–1412, 2005.
- [3] Z. Xu, "Approximate performance analysis of wireless ultraviolet links," *IEEE ICASSP Conf.*, 2007.
- [4] H. Sugiyama and K. Nosu, "MPPM: a method for improving the band-utilization efficiency in optical PPM," *J. Lightw. Tech.*, vol. 7, no. 3, pp. 465–472, 1989.
- [5] H. Zhang, W. Li, and T. Gulliver, "Pulse position amplitude modulation for time-hopping multiple-access uwb communications," *IEEE Trans. Commun.*, vol. 53, no. 8, pp. 1269–1273, 2005.
- [6] Y. Zeng, R. Green, and M. Leeson, "Multiple pulse amplitude and position modulation for the optical wireless channel," *International Conference on Transparent Optical Networks (ICTON)*, pp. 193–196, Aug. 2008.
- [7] M. Herceg, D. Zagar, and D. Galic, "Multi pulse position amplitude modulation for ultra-high speed time-hopping UWB communication systems over AWGN channel," *International Symposium on Communications, Control and Signal Processing (ISCCSP)*, May 2010.
- [8] M. Noshad and M. Brandt-Pearce, "Expurgated PPM using balanced incomplete block designs," *IEEE Commun. Lett.*, vol. 16, no. 7, pp. 968–971, 2012.
- [9] C. J. Colbourn and J. H. Dinitz, *Handbook of Combinatorial Designs*, 2nd Ed. Chapman and Hall-CRC, 2007.
- [10] Z. Xu and B. Sadler, "Ultraviolet communications: Potential and state-of-the-art," *IEEE Commun. Magazine*, vol. 46, no. 5, 2008.
- [11] L. Zeng, D. O'Brien, H. Minh, G. Faulkner, K. Lee, D. Jung, Y. Oh, and E. T. Won, "High data rate multiple input multiple output (MIMO) optical wireless communications using white LED lighting," *IEEE J. Sel. Areas Commun.*, vol. 27, no. 9, pp. 1654–1662, 2009.
- [12] M. Noshad and K. Jamshidi, "Code family for modified spectral-amplitude-coding OCDMA systems and performance analysis," *J. Opt. Commun. Netw.*, vol. 2, no. 6, pp. 344–354, 2010.
- [13] D. Zwillinger, *CRC Standard Mathematical Tables and Formulae*, 32nd Ed. Taylor and Francis, 2011.
- [14] S. S. Haykin, *Communication Systems*, 4th Ed. John Wiley & Sons, 2001.
- [15] M. Noshad and M. Brandt-Pearce, "NLOS UV communication systems using spectral amplitude coding," *Proceeding of IEEE Global communications conference (GLOBECOM)*, pp. 843–848, Houston, TX, Dec. 2011.